Biometals (2015) 28:293–306
DOI 10.1007/s10534-015-9824-1

Screen for alterations of iron related parameters in N-ethyl-N-nitrosourea-treated mice identified mutant lines with increased plasma ferritin levels

Birgit Rathkolb · Martina Klempt · Sibylle Sabrautzki · Dian Michel · Matthias Klaften · Jürgen Laufs · Reinhard Sedlmeier · Wolfgang Hans · Helmut Fuchs · Martina U. Muckenthaler · Marion Horsch · Dean R. Campagna · Mark Fleming · Martin Hrabé de Angelis · Eckhard Wolf · Bernhard Aigner

Received: 19 January 2015 / Accepted: 21 January 2015 / Published online: 31 January 2015

Abstract Iron is essential for numerous cellular processes. For diagnostic purposes iron-related parameters in patients are assessed by clinical chemical blood analysis including the analysis of ferritin, transferrin and iron levels. Here, we retrospectively evaluated the use of these parameters in the phenotype-driven Munich N-ethyl-N-nitrosourea mouse mutagenesis project for the generation of novel animal models for human diseases. The clinical chemical blood analysis was carried out on more than 10,700 G1 and G3 offspring of chemically mutagenized inbred C3H mice to detect dominant and recessive mutations leading to deviations in the plasma levels of iron-related plasma parameters. We identified animals consistently exhibiting altered plasma ferritin or transferrin values. Transmission of the phenotypic deviations to the subsequent generations led to the successful establishment of three mutant lines with increased plasma ferritin levels. For two of these lines the causative mutations were identified in the *Fth1*gene and the *Ireb2* gene, respectively. Thus, novel mouse models for the functional analysis of iron homeostasis were established by a phenotype-driven screen for mutant mice.

Keywords Iron · Ferritin · Transferrin · Mouse · ENU · Mutagenesis · Hyperferritinemia

B. Rathkolb (✉) · M. Klempt · E. Wolf · B. Aigner
Chair for Molecular Animal Breeding and Biotechnology, Department of Veterinary Sciences, and Laboratory for Functional Genome Analysis (LAFUGA), Gene Center, LMU Munich, Feodor-Lynen-Str. 25, 81377 Munich, Germany
e-mail: birgit.rathkolb@helmholtz-muenchen.de

B. Rathkolb · S. Sabrautzki · D. Michel · M. Klaften · W. Hans · H. Fuchs · M. Horsch · M. Hrabé de Angelis
Institute of Experimental Genetics, Helmholtz Zentrum München, German Research Center for Environmental Health, Neuherberg, TU Munich, Freising-Weihenstephan, Germany

S. Sabrautzki · D. Michel · M. Klaften · W. Hans · H. Fuchs · M. Horsch · M. Hrabé de Angelis
Chair for Experimental Genetics, TU Munich, Freising-Weihenstephan, Germany

J. Laufs · R. Sedlmeier
Ingenium Pharmaceuticals, Martinsried, Germany

M. U. Muckenthaler
Department of Paediatric Oncology, Hematology and Immunology, University of Heidelberg, Heidelberg, Germany

D. R. Campagna · M. Fleming
Department of Pathology, Boston Children's Hospital, Boston, MA, USA

M. Hrabé de Angelis
German Center for Diabetes Research, Neuherberg, Germany

Introduction

Iron with its two oxidation states of Fe^{2+} and Fe^{3+} is essential for basic cellular processes and necessary for the function of hemoglobin. The potential of iron to produce toxic oxygen radicals is precluded by the tight control of intestinal iron absorption as well as by iron transport and storage in a nonreactive state involving ferritin and transferrin. Clinical chemical blood analysis including ferritin, transferrin and iron as commonly used parameters is routinely applied to evaluate iron homeostasis in patients.

Ferritin is a heteropolymer of 24 subunits of heavy chain (H) and light chain (L) monomers, thereby forming a spherical cage-like structure which can hold more than 4,000 iron atoms. H ferritin is slightly larger than L ferritin. It is a ubiquitously expressed intracellular protein, which is responsible for the sequestration of potentially harmful, reactive iron thereby acting as an antioxidant protein. A small amount is released into the extracellular fluid. Plasma ferritin is mainly composed of L-ferritin and relatively iron-poor. Plasma levels have been shown to be positively correlated with total body iron stores. This parameter is therefore widely used to estimate body iron load (Beutler et al. 2002; Cohen et al. 2010). Ferritin also serves as a marker in multiple other conditions including inflammatory, neurodegenerative and malignant diseases as well as angiogenesis, but many fundamental aspects of the biology of plasma ferritin are still unclear. Ferritin production and degradation are regulated on the transcriptional and posttranscriptional level by different pathways in response to various stimuli (reviewed in (MacKenzie et al. 2008; Muckenthaler et al. 2008)). While increased ferritin levels are an indicator of moderate sensitivity and specificity for iron status, only two conditions besides iron deficiency, namely hypothyroidism and ascorbate deficiency, have been described as being associated with decreased ferritin values ((Knovich et al. 2009) and refs. therein, (Wang et al. 2010)).

Transferrin is mostly produced in hepatocytes and actively secreted into the blood. The mammalian transferrin is able to bind two iron atoms and delivers iron to cells bearing specific transferrin receptors. Serum transferrin levels rise in response to iron deficiency anemia and transferrin saturation is decreased in this condition (Andrews 2008; Bermejo and Garcia-Lopez 2009).

Humans and mice harbor genes for transferrin (*TF*, chr. 3, 133.4 Mb; *Trf*, chr. 9, 103.2 Mb), H ferritin (*FTH1*, chr. 11, 61.7 Mb; *Fth1*, chr. 19, 10.0 Mb) and L ferritin (*FTL*, chr. 19, 49.5 Mb; *Ftl1*, chr. 7, 45.5 Mb) as well as several pseudogenes of H and L ferritin (http://www.ensembl.org). Specific mutations of ferritin and transferrin are known to cause human iron disorders (Andrews 2008). Recently, genome-wide association studies were carried out using plasma ferritin, transferrin and iron for the identification of novel alleles determining iron homeostasis traits in humans (Benyamin et al. 2009; McLaren et al. 2011, 2012; Tanaka et al. 2010).

Biomedical research using mice as the animal models of choice includes the search for new alleles predisposing for or protecting against specific diseases. One strategy applied to identify novel disease-related alleles is the random chemical mutagenesis of a large number of animals followed by systematic screening for clinically relevant disease phenotypes. The most widely used mutagen is N-ethyl-N-nitrosourea (ENU) that exerts its mutagenic action on premeiotic spermatogonial stem cells. This allows the production of a large number of randomly mutant offspring from treated males. ENU predominantly induces point mutations which results in allelic series for the functional analysis of genes (Hrabé de Angelis et al. 2007). ENU mouse mutagenesis projects were established for the systematic, genome-wide, large-scale production and analysis of mouse mutants as model systems for inherited human diseases. They used appropriate routine procedures allowing the screening of large numbers of mice for a broad spectrum of parameters (Cordes 2005; Hrabé de Angelis et al. 2000; Nolan et al. 2000). Mutant lines were established for various phenotypic parameters. ENU-induced mice with the causative mutation already identified are successfully used in different areas of biomedical research ((Barbaric et al. 2007; Takahasi et al. 2007) and refs. therein).

In the Munich ENU mouse mutagenesis project, a standardized screening profile of clinical chemical blood parameters was established for the analysis of offspring of mutagenized inbred C3H mice in order to detect phenotypic variants with defects of diverse organ systems and/or changes in metabolic pathways (Gailus-Durner et al. 2005; Rathkolb et al. 2000). Here we retrospectively evaluated the generation of mutant

lines exhibiting deviations from the normal range of plasma ferritin, transferrin and iron.

Materials and methods

Mutagenesis and breeding of mice

The experiments were carried out on the inbred C3HeB/FeJ (C3H) genetic background as described (Hrabé de Angelis et al. 2000; Mohr et al. 2004). Ten-week-old male mice (=generation G0) were injected intraperitoneally with ENU (three doses of 90 mg/kg in weekly intervals) and used to produce G1 and G3 offspring which were phenotypically analysed.

The screen for dominant mutations was performed on G1 animals which were derived from the mating of the mutagenized G0 males to wild-type C3H females. G1 mice exhibiting an abnormal phenotype were again mated with wild-type C3H mice to analyse the inheritance of the observed abnormal phenotype in the G2 generation.

The screen for recessive mutations was carried out on G3 mice produced in a two-step breeding scheme from G1 mice. G1 males were mated to wild-type C3H females for the production of G2 animals. Subsequently, 6–8 G2 females were backcrossed to the G1 male to produce the G3 mice of the pedigree. The analysis of the inheritance of an observed abnormal phenotype in G3 mice was done on G5 mice. Therefore, the affected G3 mouse presumably harboring a homozygous recessive mutation was mated to a wild-type mouse for the production of the presumably heterozygous mutant G4 mice with an inconspicuous phenotype. Subsequently, the G5 mice derived from the intercross of G4 mice were tested for the abnormal phenotype. Alternatively, G5 mice derived from the backcross of a G4 mouse to the affected G3 animal were examined.

After the identification of the causative mutation, the provisional names of the established lines will be replaced according to the official nomenclature. Mouse husbandry was done in two different mouse facilities under a continuously controlled specific pathogen-free (SPF) hygiene standard according to the FELASA recommendations (Nicklas et al. 2002) (http://www.felasa.eu). All animal experiments were carried out under the approval of the responsible animal welfare authority (Regierung von Oberbayern, Germany).

Clinical chemical analysis

Ferritin and transferrin as screening parameters were included in the screening panel during later stages of the Munich ENU mouse mutagenesis project, while iron levels were measured only inconstantly in some animals of the project.

Plasma from three-month-old G1 and G3 mice was analyzed for ferritin, transferrin and iron. In the cases where altered values below or above the normal range appeared, the mice were retested after three weeks. Blood samples were obtained by puncture of the retro-orbital sinus under general short-term anesthesia. Plasma from Li-heparin treated blood was analyzed using the Olympus AU400 autoanalyzer (Olympus, Hamburg, Germany) and the reagents for human samples (Olympus). Calibration and quality control were performed according to the manufacturer's protocols. Due to methodological changes in the ferritin test kit during the ongoing project, ferritin values were measured in the first time period with kit A and in the second time period using kit B (see Table 1). Measurements of the animals in the first test were always done on 1:2 diluted samples, resulting in about 4 % of measured ferritin values and 9 % of measured transferrin values in diluted samples below the lower limit of the linear measurement range. The samples used for the retests and the samples collected from offspring of test-crosses or maintenance breeding of mutant lines were measured either undiluted or diluted appropriately to achieve values within the linear range.

In addition, the clinical chemical screen of plasma samples included the measurement of substrates (cholesterol, creatinine, glucose, total protein, triglycerides, urea, uric acid), electrolytes (calcium, chloride, inorganic phosphorus, potassium, sodium) and enzyme activities (alanine aminotransferase, aspartate aminotransferase, alkaline phosphatase, α-amylase, creatine kinase).

Analysis of hematological parameters was done using an Animal Blood Counter (Scil, Viernheim, Germany) validated by the manufacturer for the analysis of mouse blood. In EDTA-treated blood, the following hematological parameters were directly measured: red blood cells: hemoglobin (HGB), mean corpuscular volume (MCV), red blood cell count (RBC); white blood cells: white blood cell count (WBC), platelet count (PLT). The parameters

hematocrit (HCT), mean corpuscular hemoglobin (MCH) and mean corpuscular hemoglobin concentration (MCHC) were subsequently calculated using the parameters described above (Klempt et al. 2006).

Linkage analysis of the causative mutation and sequence analysis of candidate genes

Two backcross generations were produced using C57BL/6 mice as the second inbred strain. In mutant lines harboring a dominant mutation, phenotypic mutant C3H males were mated to female C57BL/6 mice. The resulting G1 mice were analyzed for heterozygous phenotypic mutants who were again bred to C57BL/6 mice. In mutant lines harboring a recessive mutation, homozygous phenotypic mutant C3H males were mated to C57BL/6 mice, and the resulting G1 hybrid mice were intercrossed. In both cases, the G2 offspring were phenotypically classified into mice exhibiting normal or altered plasma ferritin levels. After sacrifice, tissue samples were collected for subsequent DNA isolation.

Tail clip samples were incubated overnight in a lysis buffer consisting of 10 mM Tris–HCl (pH 8.0), 1 % (w/v) SDS, 50 mM EDTA and 300 µg/ml Proteinase K (Sigma-Aldrich, Taufkirchen, Germany). Automated DNA extraction from the lysates was performed using the AGOWA Mag Maxi DNA Isolation Kit (AGOWA, Berlin, Germany). For linkage analysis, a genome-wide mapping panel consisting of microsatellite and/or single nucleotide polymorphism (SNP) markers was applied. The markers used are available upon request. Analysis of this panel was performed using MassExtend, a MALDI-TOF high-throughput genotyping system supplied by Sequenom (San Diego, CA, USA). Chromosomal positions of markers and genes are according to the GRCm38 mouse assembly, January 2014 (http://www.ensembl.org).

Candidate genes localized within the determined chromosomal regions were selected by using the known phenotypes as selection criteria in the bioinformatic analysis (http://omicspace.riken.jp/PosMed/) and subsequently examined by sequence analysis.

Analysis of gene expression of line FER001

Spleen and liver were collected from five male phenotypically mutant mice and six male wild-type littermates of line FER001 at an age of seven months. Samples were stored in RNA-later at 4 °C for three days before freezing at −20 °C according manufacturer's protocol (Qiagen). Total RNA was extracted and gene expression levels of iron metabolism related genes were analyzed on 'IronChips' (Muckenthaler et al. 2003) by applying pooled samples of total RNA from liver and spleen of mutant compared to wild-type mice.

Immunoblot analysis of line FER003

Liver tissue was manually lysed in modified RIPA buffer (50 mM Tris [pH 7.5], 150 mM NaCl, 1 % NP-40, 0.5 % sodium deoxycholate, 0.1 % SDS). Cell debris was removed by centrifugation. Total tissue protein (50 µg) was diluted in 2 × Laemmli buffer (0.2 M DTT final), boiled, and subjected to electrophoresis through 10 % polyacrylamide gels. The proteins were transferred onto nitrocellulose membranes, and immunoblot analysis was performed using mouse anti-IREB2 (1:1,000, Rick Eisenstein, Univ. of Wisconsin-Madison). Blots were incubated with anti-rabbit secondary antibody conjugated to horseradish peroxidase (1:10,000) and then subjected to chemiluminescence (Amersham ECL) according to the manufacturer's protocols.

Statistical analysis

The statistical analysis of the data was carried out using the software programs Microsoft Excel 2000 (Microsoft, Redmond, WA) and Sigma Stat 3.1. Values are presented as medians, and 95 % and 90 % ranges unless stated otherwise.

Results and discussion

Normal plasma values of ferritin, transferrin and iron in C3H mice

In the Munich ENU mouse mutagenesis project, the plasma parameters ferritin, transferrin and iron were analyzed during a time period of one (for iron) to three (for ferritin and transferrin) years of the Munich ENU mouse mutagenesis project. The baseline values for clinical chemistry parameters screened were determined in about 200 male and 200 female three-month-

Table 1 Retrospective analysis of the normal range of plasma parameters for iron homeostasis in three-month-old C3H mice of the Munich ENU project

Parameter	Unit	Olympus kit[a]	Sex	n[b]	Median	95 % range	90 % range
Ferritin	µg/l	OSR6150, Kit A	m	3,153	46	17–86	24–77
			f	1,748	62	26–118	33–101
		OSR6150, Kit B	m	3,894	24	10–42	13–38
			f	1,944	27	13–46	16–42
Transferrin	mg/dl	OSR6152	m	7,028	175	139–242	144–231
			f	3,696	177	138–250	144–239
Iron	µg/dl (µmol/l)	OSR6186	m	314	155 (28)	104–238 (19–43)	112–211 (20–38)
			f	147	174 (31)	105–287 (19–51)	112–249 (20–45)

m/f, Males/females

[a] Linear measurement ranges for the Olympus AU400 autoanalyzer (Olympus, Hamburg, Germany) and the reagents for human samples are 8–450 µg/l for ferritin, 75–750 mg/dl for transferrin and 10–1,000 µg/dl (2–179 µmol/l) for iron

[b] G1 and G3 offspring of ENU-treated mice for the dominant and recessive screen. About 60 % of the analyzed mice were males

old wild-type C3H mice (Klempt et al. 2006) and the 95 % range of the values was defined as the normal range (Loeb and Quimby 1999). According to the defined normal range, abnormally low and high values were determined in the G1 and G3 offspring of ENU-mutagenized mice. On the one hand, the defined normal range must allow to phenotypically detecting animals with heritable defects leading to altered plasma parameter levels. On the other hand, it must exclude smaller variations from the mean level which are not suitable for breeding a mutant line over several generations according to the phenotypic variations.

As the Munich ENU project was carried out in two different mouse facilities over a time period of many years, we re-evaluated the cut-off levels for ferritin, transferrin and iron in retrospect for the present study. Plasma values of more than 10,700 male and female G1 and G3 offspring of ENU-mutagenized mice were analyzed for ferritin and transferrin over a time period of three years, whereas a subgroup of only 461 G1 and G3 offspring were analyzed for plasma iron values (Table 1). Less than 1 % of the G1 and G3 mice were expected to be primarily altered by ENU-induced mutations for a given blood parameter. Thus, the 95 % range of the values determined in the large resource of animals should also comply with the successful detection and breeding of mutant animals with altered plasma values.

Ferritin values obtained with the test kit A in the first time period were remarkably different from those obtained with the test kit B in the second time period. Therefore kit-specific reference ranges were calculated for the two time periods (Table 1). Statistical evaluation showed lower plasma ferritin values in males compared to females ($p < 0.001$), while there was no influence of the facility. For plasma transferrin, significant effects ($p < 0.001$) of sex in facility one and of the mouse facility for both sexes were indicated by statistical analysis, although the differences were very small (Fig. 1). The latter effect might be due to the fact that different diets were fed in the two facilities. In addition, periodical shifts were observed in transferrin values, which were independent of sample source and sex of the animals tested (data not shown) and therefore most likely due to technical effects (e.g. different lots of antibodies used in the test kit). This variation of the values hampered the identification and confirmation of variants during the screen.

Few data on plasma ferritin, transferrin and iron have been published from other projects which also used C3H mice (Champy et al. 2008). They varied widely thereby indicating that project-specific controls are indispensable.

Subsequently, deviations in plasma ferritin, transferrin and iron values were defined in our retrospective analysis for mice showing values below or above the limits of the 95 % range in two measurements of a three-week interval. For the retrospective identification of mice showing outlier values, separate

calculation of the normal plasma values was done for both mouse facilities involved and per every year of the study for ferritin and iron, and for every time period showing distinct measurement ranges in case of transferrin (data not shown).

Screening for ENU-induced phenotypic variants showing altered plasma values of ferritin, transferrin or iron

In the Munich ENU mouse mutagenesis project, more than 10,700 three-month-old G1 and G3 offspring of ENU-treated mice were screened for deviations in plasma ferritin and transferrin presumably caused by dominant or recessive mutations, respectively. The examined offspring included more than 5,100 G1 mice and 5,500 G3 mice. Separate calculation of the 95 % ranges for each of the two ferritin test kits and for each period with distinct transferrin ranges retrospectively identified in total 866 mice (8 %) with values above or below this range in the first measurement, including 26 animals (0.2 % of all mice screened, 3 % of mice showing deviant values) showing altered values for both parameters.

However, only a small part (n = 181) of these animals was retested a second time, leading to the identification of 53 animals (30 males/23 females; 29 % of mice retested) as phenotypic variants showing increased or decreased values in two blood samples taken in a three-week interval: ferritin high in five males from the dominant screen and 28 animals (12 males/16 females) from the recessive screen; ferritin low in one male from the dominant screen; transferrin high in nine mice (5 males/4 females) from the recessive screen; transferrin low in four animals (2 males/2 females) from the dominant screen and five mice (4 males/1 female) from the recessive screen; and one male phenotypic variant from the recessive screen showing both increased plasma ferritin and transferrin levels.

In total about half of the abnormal values of the first measurement were confirmed in the second measurement with the exception of low ferritin values. Retests of 74 mice with low ferritin values in the first measurement confirmed this phenotype in only one animal. This might indicate a poor reliability of low ferritin values or might be due to secondary effects that occurred due to the first blood withdrawal challenging regulatory mechanisms of iron metabolism.

The 43 G3 phenotypic variants from the recessive screen were offspring of 17 different G1 males, but 30 of these 43 G3 phenotypic variants were produced with only four G1 males. Offspring of the same G1 animal showing deviations in the same phenotypic parameter were assumed to carry the identical mutation.

One of these mutant pedigrees carrying a recessive mutation was preliminary named CCH001 and contained phenotypic variants also showing abnormal values for several plasma enzyme activities (alanine aminotransferase, aspartate aminotransferase, alkaline phosphatase, α-amylase) and hematological parameters. The homozygous mutants were phenotypically defined if at least three of the plasma enzyme activities were altered (Aigner et al. 2009a, 2011). Re-analysis of plasma ferritin as secondary parameter in the phenotypic mutants of this line revealed values above the cut-off level in 50 % of the animals (n = 22 of 44).

Search for mice with abnormal plasma iron values in the more than 450 analyzed G1 and G3 offspring was negative. Use of the less stringent 90 % range as normal range led to the detection of three phenotypic variants (one male and two females) showing increased plasma iron levels which included two animals with abnormal plasma transferrin levels. However, these animals were not further analyzed.

Establishment of mutant lines showing increased plasma ferritin values

Selected phenotypic variants were tested for the inheritance of the deviations in plasma ferritin or transferrin values during the ENU project. Therefore the affected parameter was analyzed on G2 offspring from the mating of G1 phenotypic variants to wild-type mice in the screen for dominant mutations, and on G4 × G3 backcross offspring after breeding G3 phenotypic variants to wild-type mice in the screen for recessive mutations. Sperm was cryopreserved from male phenotypic variants which were not mated to enable later inheritance testing wherever it was possible. A heritable altered plasma level was diagnosed when offspring of the phenotypic variants showed values below or above the cut-off level in two measurements of a three-week interval.

In total 18 phenotypic variants with altered plasma ferritin levels and seven phenotypic variants with altered plasma transferrin values were mated, but eight

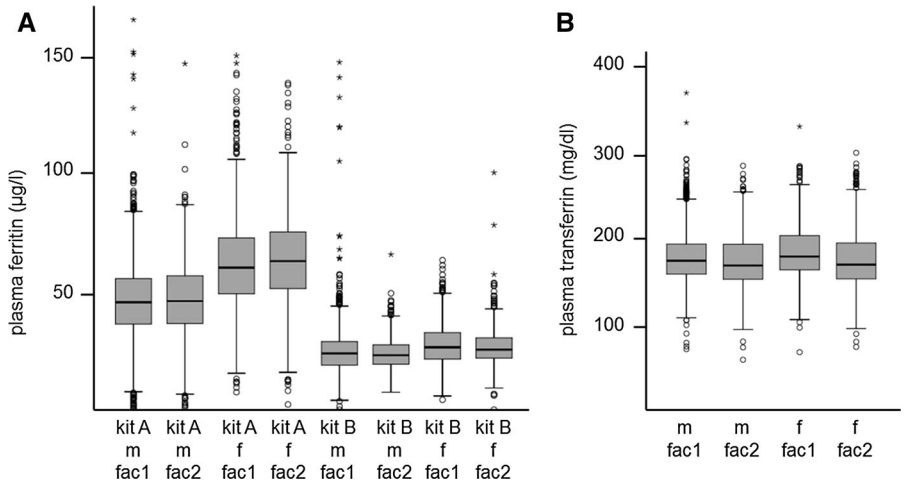

Fig. 1 *Boxplots* indicating median, quartiles, and whiskers with 1.5 × the box length thereby expected to include the 95 % range of **a** plasma ferritin values (µg/l) measured with the two test kits *A* and *B* and of **b** plasma transferrin (mg/dl) in male (m) and female (f) G1 and G3 animals from facility 1 (fac1) and 2 (fac2). The analysis (SPSS Statistics 19, http://www.spss.com) includes data from 5,638 males and 2,321 females of facility 1 and 1,428 males and 1,379 females of facility 2. *Dots*: values outside the range of 1.5 × the box length; *stars*: values outside the range of 3 × the box length. *t* test of the groups for plasma ferritin: sex: $p < 0.001$. *t*-test of the groups for plasma transferrin: sex in facility 1: $p < 0.001$; mouse facility: $p < 0.001$

of these matings (4 for ferritin and 4 for transferrin) did not produce any offspring.

Phenotypic analysis of the offspring was carried out for 14 of the retrospectively identified G1/G3 phenotypic variants showing deviations for plasma ferritin. Five phenotypic variants did not give rise to phenotypic mutant offspring. Nine G3 phenotypic variants with increased plasma ferritin levels showed the inheritance of the altered phenotype to the offspring. Seven of the nine G3 phenotypic mutants were derived from the same G1 male and, therefore, were suggested to harbor the same causative mutation. Thus, we produced three independent ENU-induced mutant lines (FER001, FER002, FER003) with increased plasma ferritin levels (Table 2).

In addition, phenotypic analysis of the offspring was carried out for three of the retrospectively identified G1/G3 phenotypic variants showing deviations for plasma transferrin. However, all three phenotypic variants did not give rise to phenotypic mutant offspring. The lack of offspring from phenotypic variants showing the mutant phenotype likely indicated the absence of a genetic cause for the altered phenotype.

For the establishment of ENU-induced mutant lines with deviations in plasma cholesterol, glucose and urea as well as plasma enzyme activities in the Munich ENU mutagenesis project we obtained similar results. For these parameters breeding of more than five phenotypic variants was necessary to establish one mutant line with increased plasma levels, whereas transmission of decreased levels from the phenotypic variants to the offspring was observed in more than every third mating [(Aigner et al. 2009a) and refs. therein].

Re-evaluation of the three G1 animals which were used to produce the G3 phenotypic variants leading to the mutant lines FER001, FER002 and FER003 with increased plasma ferritin levels revealed that they were analyzed in the clinical chemical screen before the novel plasma parameters ferritin, transferrin and iron were used. Thus, there were no data for these parameters in these three G1 animals.

To retrospectively determine, if the causative mutation in the three G1 animals is dominant or recessive, we re-checked the phenotypic data of their G3 offspring including animals which were measured only once. In the breeding scheme used for the generation of the G3 generation, 50–75 % G3 phenotypic variants are expected to occur in the case of a dominant mutation, and 0–25 % G3 phenotypic variants in the case of a recessive mutation. The G1 ancestor of mutant line FER001 gave rise to 80 % (n = 12 of 15) G3 phenotypic variants, the G1 animal

leading to mutant line FER002 gave rise to 70 % (n = 14 of 20) G3 phenotypic variants, and the G1 animal leading to mutant line FER003 gave rise to 21 % (n = 4 of 19) G3 phenotypic variants. Therefore, the causative mutations in lines FER001 and FER002 were suggested to be dominant, and the causative mutation in line FER003 was suggested to be recessive. This also explained the high numbers of G3 phenotypic variants derived from the two G1 mice leading to the lines FER001 and FER002.

Breeding of the mutant lines over several generations with matings of homozygous mutant, heterozygous mutant and wild-type animals confirmed the occurrence of a dominant mutation in lines FER001 and FER002 with viable and fertile homozygous mutant offspring, and of a recessive mutation in line FER003 according to the Mendelian ratio (Table 2). The lines were bred for at least four generations without losing the altered phenotype which indicated the monogenic cause of the abnormal phenotype. The appearance of differences in the plasma ferritin phenotypes between homozygous mutant and heterozygous mutant animals in lines FER001 and FER002 was not investigated. The phenotypic mutants of all three lines FER001, FER002 and FER003 showed no correlation to deviations in plasma transferrin or iron outside the defined 95 % range (not shown).

Further hematological and morphological analysis of the mutant lines established

For the evaluation of the hematological parameters in the phenotypic mutants, the physiologic range of the values was also analyzed in retrospect including the data of more than 15,000 animals. The 95 % range of the parameters was as follows: HGB (g/dl): 12.9–17.0 for males and 12.6–17.1 for females; RBC ($\times 10^6$/µl): 7.8–10.6 and 7.5–10.4; MCV (fl): 47–52 and 47–53; HCT (%): 38.4–52.9 and 37.5–52.2; MCH (pg): 14.7–18.4 and 14.9–18.9; MCHC (g/dl): 29.5–37.7 and 29.5–38.3; WBC ($\times 10^3$/µl): 1.5–7.8 and 1.6–7.8; PLT ($\times 10^3$/µl): 346–844 and 313–824 (Aigner et al. 2011).

Analysis of the hematological parameters HGB, RBC, MCV, HCT, MCH, MCHC, WBC and PLT in the phenotypic mutants with increased plasma ferritin levels compared to the phenotypic wild-type littermates in the lines FER001 and FER002 observed no hematological values outside the defined 95 % range which were correlated to the increased plasma ferritin. However, the lack of abnormal hematological values in phenotypic mutants does not exclude the existence of significant differences in these parameters between mutant and wild-type mice. This has to be analyzed after the detection of the causative mutation. In line FER003, the G3 phenotypic mutant as founder of this line showed decreased levels of HGB, MCV, MCH and MCHC. Phenotypic mutant offspring also showed the deviations of one or more of these parameters (not shown).

General morphological analysis of the mutant lines revealed that increased plasma ferritin levels in the phenotypically mutant mice of line FER001 were associated with a lighter colour of the upper incisors (Fig. 2). This was not seen in lines FER002 and FER003.

Analysis of expression of iron metabolism related genes in line FER001

Gene response patterns of iron-related genes were analysed in the liver and spleen of heterozygous FER001 mutant mice compared to wild-type littermates. A large number of gene expression changes could be detected that in average ranged between 1.5 and 3.3-fold (Fig. 3). Hepatic mRNA expression of toll-like receptor 8 and tyrosinase showed a more than 7-fold change in mutant mice compared to controls. Fifteen differentially regulated genes showed similar expression changes in the liver and spleen. Although the only detectable phenotype in the FER001 mouse line was the colour change of the teeth that was associated with high ferritin levels, the causative mutation seems to have effects on the expression of several genes related to iron metabolism.

Only a mild downregulation of ferritin heavy chain 1 (*Fth1*)mRNA was detectable in the spleen of mutant mice but not in liver. In addition, ferritin light chain (*Ftl1*) mRNA was not differentially expressed in the liver and the spleen. Therefore, high plasma ferritin levels in mutant FER001 mice are not a consequence of altered mRNA-expression of the ferritin genes.

Analysis of the causative mutations in the mutant lines FER001, FER002 and FER003

Mouse breeding for the linkage analysis to identify the chromosomal site of the causative mutation was

Table 2 Mutant lines showing increased plasma ferritin values derived from the Munich ENU mouse mutagenesis project

Line	Mode of inheritance	Mating	Offspring: n (m/f)	Altered plasma values: total (m/f)			Generations established
				N	%	Range/median[a] (μg/l)	
FER001	Dominant	het × wt	98 (47/51)	48 (19/29)	49	166–370/301	6
FER002	Dominasnt	hom × hom/het	44 (26/18)	44 (26/18)	100	210 to >450/346	4
FER003	Recessive	hom × het	10 (5/5)	5 (3/2)	50	104 to >450/> 450	4
		het × het	34 (16/18)	8 (6/2)	24	156–426/307	

The plasma ferritin levels of the mating "hom × het" of line FER003 were measured with test kit A; all other measurements were carried out using test kit B

m/f, Males/females

Hom Homozygous mutant, *het* heterozygous mutant, *wt* wild-type

[a] According to the linear measurement range for ferritin (8–450 μg/l), values >450 μg/l were not exactly indicated

carried out in the lines FER001 and FER002, harboring dominant mutations, and FER003 carrying a recessive mutation. In the Munich ENU project, wild-type C57BL/6 mice were normally used as the second inbred strain. Although comparative analysis of plasma ferritin levels in a small number of animals of various inbred strains detected increased mean levels both in male and female C57BL/6 mice compared to C3H mice used in this study (Aigner et al. 2009b), detection of phenotypic mutant F1 hybrid mice as well as the classification of the N2 mice in phenotypic mutants and wild-type littermates were possible in both approaches.

Using genome-wide polymorphic DNA markers, the chromosomal position of the causative mutations in both lines FER001 and FER002 was mapped to the proximal region of chromosome 19 (3.6–14.7 Mb in line FER001, and 0–25.1 Mb in line FER002), while the causative mutation in line FER003 was mapped to chromosome 9 (32.7–64.5 Mb) (according to the GRCm38 mouse assembly, January 2014, http://www.ensembl.org) (Fig. 4). The probability of the existence of confounding non segregating mutations in the mapped chromosomal regions (see above) is $p = 0.064$ for line FER001, $p = 0.092$ for line FER002, and $p = 0.087$ for line FER003 (Keays et al. 2007). The loci identified in genome-wide association studies for iron homeostasis traits in humans (Benyamin et al. 2009; McLaren et al. 2011, 2012; Tanaka et al. 2010) did not match to the mapped chromosomal regions.

For the lines FER001 and FER002, bioinformatic analysis (http://omicspace.riken.jp/PosMed/) of the determined chromosomal regions identified 429 and 521 Ensembl genes, respectively. Search for candidate genes in these regions by using bioinformatic tools (http://omicspace.riken.jp/PosMed/) identified ferritin heavy chain 1 (*Fth1*) at 10.0 Mb. *Fth1* homozygous knockout mice have been described to show complete prenatal lethality, whereas *Fth1* heterozygous knockout mice are described with an increased L- to H-subunit ratio and highly increased plasma L ferritin levels together with unchanged plasma iron levels (Ferreira et al. 2001). In humans, several point mutations in the regulatory region of the ferritin light chain gene (*FTL*) led to a high constitutive, poorly regulated L ferritin synthesis resulting in hyperferritinemia (Beaumont et al. 1995; Girelli et al. 1995) (http://www.ncbi.nlm.nih.gov/omim). Ferritin light chain deficiency in contrast, has been found to be associated with undetectable plasma ferritin levels and H homopolymer ferritin formation associated with seizures and atypical restless leg syndrome in a human patient (Cozzi et al. 2013). In addition, altered ferritin expression in papillary layer cells of *Nfe2l2* homozygous knockout mice is associated with decolourization of teeth as it is observed in mutant mice of line FER001, due to reduced iron deposition in the enamel layer (Yanagawa et al. 2004).

In line FER001, compared to the sequence of wild-type C3H controls, sequence analysis of the promoter region, the coding sequences, the 5′ UTR including the iron response element (IRE) sequence, the 3′ UTR and the exon–intron-boundaries of *Fth1* (182 aa) in phenotypically heterozygous mutant mice revealed a T to C point mutation at nt 94 of the coding sequence

Fig. 2 Phenotypically heterozygous mutant mice with increased plasma ferritin levels of line FER001 showed a lighter colour of the upper incisors compared to wild-type C3H controls

A

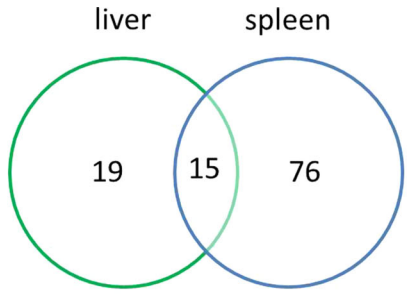

B

Liver			both		Spleen							
AFC	Gene name	AFC	Gene name	AFC	Gene name	AFC	Gene name	AFC	Gene name	AFC	Gene name	AFC
-1.85	*Acas2*	-2.32	*Alas1*	-1.61	*Psap*	-3.12	*Urod*	-1.90	*Fcna*	-1.52	*Fnbp3*	1.85
-1.75	*Hspa1a (short)*	-1.91	*Eno1*	-2.18	*Ltf*	-2.99	*Ccnf*	-1.87	*Trappc4*	-1.50	*Klra6*	1.85
-1.56	*Akr1b8 (bad)*	-1.65	*Gapd*	-1.80	*App*	-2.74	*Aco1*	-1.86	*Sfxn1*	-1.50	*BC021442*	1.88
-1.55	*Psmc4*	-1.54	*Hspa8*	-1.56	*Actb*	-2.60	*1110012O05Rik*	-1.82	*MTB-Snrpb2*	1.50	*Hnrpdl*	1.91
-1.53	*Arg1*	-1.59	*Hspa5*	-1.54	*Gsn*	-2.55	*Cotl1*	-1.82	*4833418A01Rik*	1.52	*Clock*	1.94
1.61	*Tlr3*	1.51	*Tlr4 (short)*	1.95	*Stmn1*	-2.54	*Prnp*	-1.80	*Trpc2 (form 2)*	1.53	*Tfrc*	1.95
1.63	*Il9r (long)*	1.64	*Tlr4*	2.43	*App (short)*	-2.50	*Hmbs (bad)*	-1.76	*Bcl2*	1.54	*Tceb1*	1.96
1.65	*Cd160 (long)*	1.69	*Cdc14a*	1.60	*Calr*	-2.40	*Hspa9a*	-1.67	*Abcb7 (short)*	1.55	*Pnpt1*	2.00
1.65	*Sfxn5*	1.59	*Rpl32*	1.71	*Pah*	-2.39	*Bcl2l1*	-1.67	*2610312B22Rik*	1.55	*Ddx5*	2.01
1.66	*Vamp3*	1.74	*Gls*	2.50	*Cct7*	-2.38	*Txn2*	-1.61	*Hspca*	1.56	*Trpm7*	2.03
1.80	*Slc30A3*	1.80	*Csnb*	1.81	*Trf*	-2.32	*Hmbs*	-1.60	*Ireb2*	1.58	*Bnip3l*	2.06
1.83	*Cd160*	1.91	*Ccl11*	1.67	*Hba-a1*	-2.31	*Idh3g*	-1.59	*Rbm8a*	1.58	*Capza2*	2.12
1.90	*Figf*	2.04	*Slc30a4*	1.93	*Mpo*	-2.14	*Prkaca*	-1.59	*Sepp1*	1.59	*Tmsb4x*	2.16
1.92	*Slc39A2*	3.25	*Hfe (long 1)*	1.56	*Ctsd*	-2.11	*Ldh1*	-1.58	*Sec61g*	1.60	*Dnaja1*	2.18
1.99	*Mmp3*	7.46	*Tyr*	1.61	*Got2*	-1.99	*Slc11a2*	-1.57	*Trpc1*	1.68	*Acox3*	2.57
2.15	*Sfxn3*				*Aplp2*	-1.99	*Fth1*	-1.56	*Selp*	1.70	*Cox7b*	2.67
2.49	*Prkr*				*Lcn2*	-1.99	*Hmox1*	-1.55	*Acox2*	1.71		
2.75	*Tlr9 (long)*				*Akr1a4*	-1.97	*Ran*	-1.55	*Cul3 long form*	1.71		
7.02	*Tlr8*				*Kif20a*	-1.94	*Slc7a7*	-1.54	*5730454B08Rik*	1.76		
					Txnrd2	-1.93	*Bat1a*	-1.53	*Abce1*	1.79		

Fig. 3 Number (**a**) and list (**b**) of genes differentially expressed in liver and spleen of phenotypically heterozygous mutant and wild-type FER001 mice, with an average fold change (AFC) of more than 1.5

(exon 1) leading to the amino acid exchange from serine (TCC) to proline (CCC) at position 32 (*Fth1*^{S32P}). The results of the sequence analysis were confirmed by establishing a PCR–RFLP for the mutation (Fig. 5a).

Decolourization of teeth has not been described for the already published *Fth1* heterozygous knockout mice which may be due to the lacking analysis of this phenotypic parameter, to differences in the level of reduction of iron deposition in the teeth, or to differences

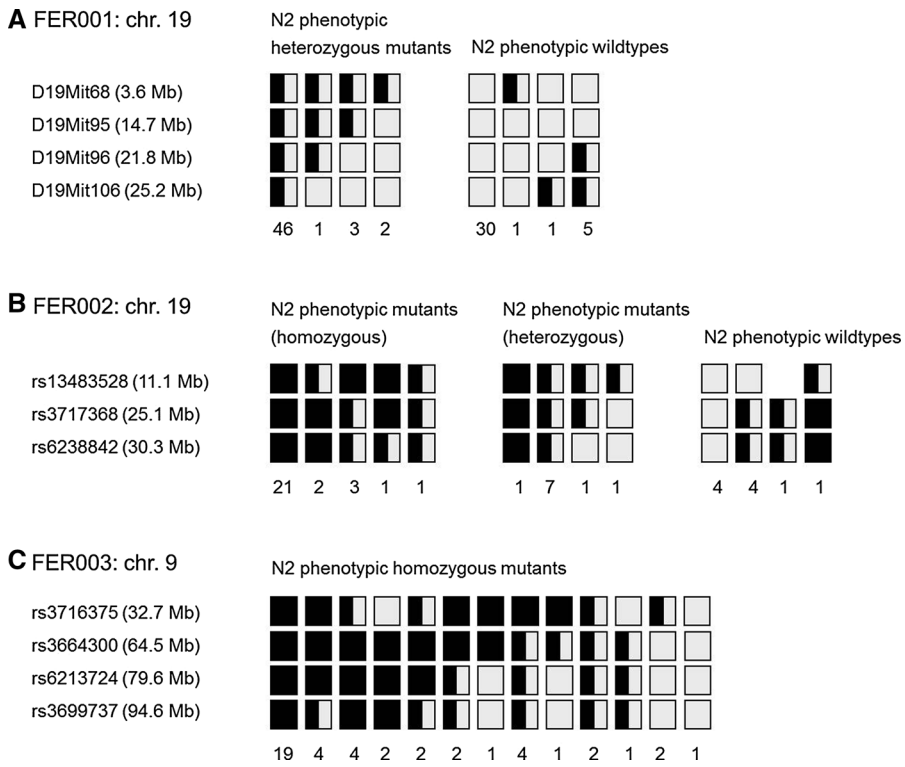

Fig. 4 Linkage analysis of the causative mutation on chromosome 19 (61 Mb) in the mutant lines FER001 (**a**) and FER002 (**b**), and on chromosome 9 (125 Mb) in the mutant line FER003 (**c**). Position of the polymorphic DNA markers according to the GRCm38 mouse assembly, January 2014 (http://www.ensembl.org). *Squares* show the genotype for the respective marker: *black*: C3H/C3H; *black and grey*: C3H/C57BL/6; *grey*: C57BL/6/C57BL/6. *Numbers* below the columns of *squares* indicate the numbers of N2 animals phenotyped. The N2 animals were produced by breeding phenotypically heterozygous mutants twice to C57BL/6 mice for line FER001 harbouring a dominant mutation. For line FER002 harbouring a dominant mutation and for line FER003 harbouring a recessive mutation, phenotypic C3H mutants were mated to C57BL/6 mice, and the resulting G1 hybrid mice were intercrossed. The N2 phenotypic mutants for line FER002 were attempted to classify in heterozygous mutants and homozygous mutants according to the increased plasma ferritin level

in the ferritin expression in the teeth compared to *Nfe2l2* knockout mice. In addition, *Fth1* heterozygous knockout mice have been described to mimic the protein profile for iron management in the adult brain as seen in human neurodegenerative disorders leading to oxidative stress (Thompson et al. 2003). Thus, further analyses in our novel established $Fth1^{S32P}$ mutant mice should include the characterization of homozygous mutants as well as further organ analysis including the brain. Furthermore our results indicate, that specific *Fth1* mutations like certain mutations in the ferritin light chain could be a cause of familial hyperferretinemia (Kannengiesser et al. 2009).

In line FER002, sequence analysis of the same sequences of *Fth1* as analyzed in line FER001 (see above) in phenotypically heterozygous or homozygous mutant mice revealed no difference compared to the sequence of wild-type C3H controls. In addition, no difference was found in the sequence analysis of the complete intron 1, thereby completing the sequence analysis of all *Fth1* intronic sequences.

For the line FER003, bioinformatic analysis (http://omicspace.riken.jp/PosMed/) of the determined chromosomal region of chromosome 9 (32.7–64.5 Mb) identified 549 Ensembl genes. The iron responsive element binding protein 2 (*Ireb2*) gene on chromosome 9 (54.9 Mb) was chosen as a candidate for sequence analysis. IREB2 deficient mice have been shown to exhibit comparable phenotypes as seen in mutants of line FER003 (Cooperman et al. 2005; Galy et al. 2005). Sequence analysis of *Ireb2* (963 aa) revealed a truncating nonsense mutation due to a point mutation c. 2,467 C > T, thereby leading to the mutation *Ireb2* Q823X (Fig. 5b).

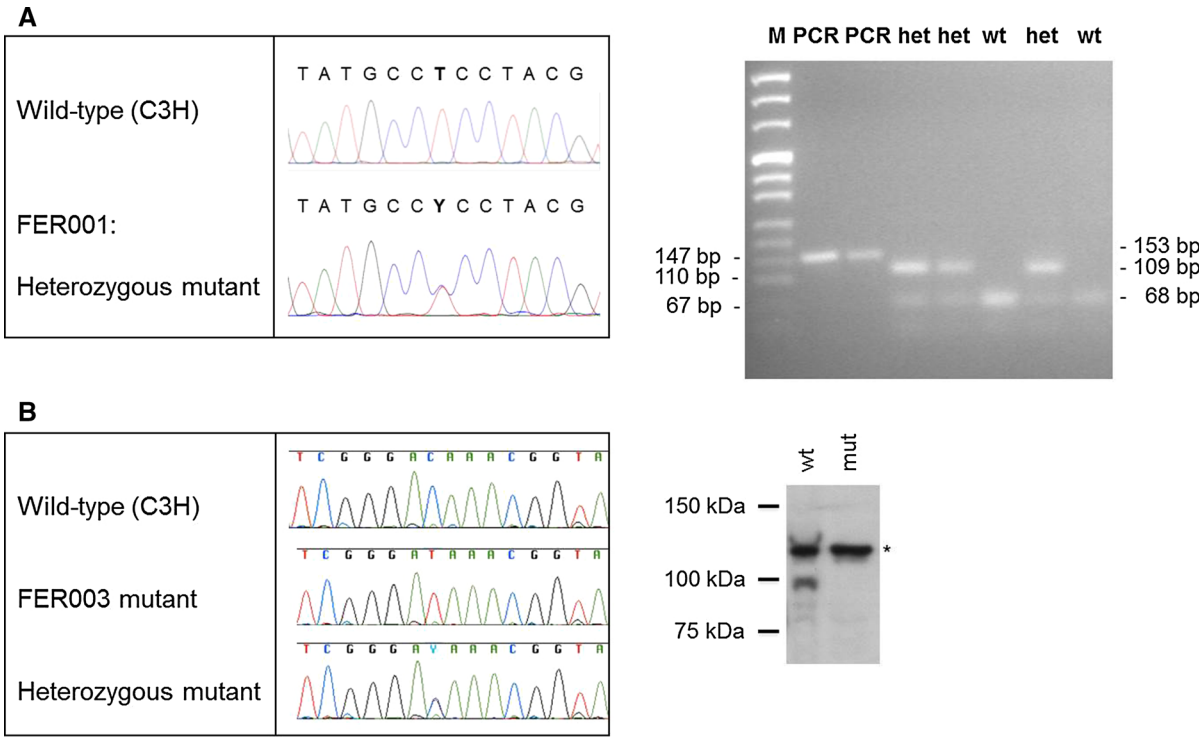

Fig. 5 Analysis of the causative mutations in the lines FER001 (**a**) and FER003 (**b**). **a** Sequence analysis of *Fth1* in line FER001. *Left*: Heterozygous mutant mice show a T to C point mutation at nt 94 of the coding sequence leading to the amino acid exchange $Fth1^{S32P}$ (*bold*). *Right*: PCR–RFLP for the mutation. Unrestricted PCR products (PCR; fw primer: 5′-gcaagtgcgccagaactacc-3′, rv primer: 5′-caagtggccctgaggaggc-3′) show a length of 153 bp. MnlI restriction leads to a 68 bp signal and smaller bands (not visible) in homozygous wild-type mice (*wt*), whereas an additional 109 bp signal is seen in heterozygous mutants (*het*). **b** Sequence analysis of *Ireb2* in line FER003. *Left*: Homozygous mutant mice show a C to T point mutation at nt 2,467 of the coding sequence leading to the amino acid exchange $Ireb2^{Q823X}$. *Right*: Immunoblot analysis of IREB2 in wild type and homozygous mutant whole liver lysates. *Asterisk* denotes non-specific band

Mutant lines with deviations of plasma ferritin, transferrin or iron derived from other phenotype-driven ENU projects

Major centers performing phenotype-driven ENU mutagenesis-based projects used clinical chemical screens for the generation of novel mutant mouse models (Cordes 2005). Search for defined phenotypes in published chemically induced (ENU) mutants (as of 29.01.2014) of the "phenotypes and alleles" database in the Mouse Genome Informatics website (http://www.informatics.jax.org/searches/allele_form.shtml) revealed 2,963 alleles and 2,326 genes/markers. Among them, 793 alleles and 635 genes/markers were described with phenotypes influencing "hematopoietic" and/or "homeostasis/metabolism" and/or "liver/biliary" pathways.

However, plasma parameters associated with iron homeostasis were rarely used in the primary clinical chemical screens. Detection of altered plasma iron levels in a G3 mouse led to the production of a mutant line with a recessive mutation where the homozygous mutants showed increased plasma iron levels and increased plasma ferritin levels. A point mutation in the transferrin receptor 2 (*Tfr2*) gene was observed as the causative mutation (http://www.informatics.jax.org; http://mutagenetix.scripps.edu).

Primary screens for other parameters like dysmorphology and/or hematology/anemia resulted in the generation of ENU-induced mutant lines where deviations in iron homeostasis were found as essential phenotype in the subsequent clinical chemical analyses of the lines, e.g. increased serum ferritin levels and hypoferremia in a dominant negative mutation of the iron exporter ferroportin (*Slc40a1*) gene (Zohn et al. 2007), hypoferremia in three recessive mutant alleles of *Tmprss6* (Du et al. 2008) (http://www.informatics.jax.org; http://mutagenetix.scripps.edu) and in *Atp4a*

mutants (Krieg et al. 2011), decreased plasma iron levels combined with increased liver iron levels in *Cp* mutants (http://www.informatics.jax.org; http://mutagenetix.scripps.edu), increased plasma iron levels in a recessive mutation of *Spta1* (Robledo et al. 2010) and in *Trpc3* mutants (http://www.informatics.jax.org), normal serum iron levels but increased total iron binding capacity in a recessive mutation of *Steap3* (Lambe et al. 2009), as well as increased kidney, liver and/or spleen iron levels in mutations of *Ank1* (Greth et al. 2012; Huang et al. 2013; Rank et al. 2009; Yuki et al. 2013) and *Klf1*^{Nan} (Heruth et al. 2010; Siatecka et al. 2010).

Conclusions

In this study, we retrospectively evaluated the use of plasma ferritin, transferrin and iron in the clinical chemical blood analysis of the Munich ENU mouse mutagenesis project to detect dominant and recessive mutations leading to deviations in iron homeostasis. Analysis of more than 10,500 G1 and G3 mice derived from ENU-mutagenized G0 males revealed more than 50 phenotypic variants showing abnormally high or low values for one or more of these parameters in two consecutive tests. To date, three mutant lines with increased plasma ferritin levels were established. Successful linkage analysis was carried out for these lines, and the causative mutation was identified in line FER001 in the gene *Fth1* and in line FER003 in the gene *Ireb2,* while the causative mutation in line FER002 remains to be discovered. The use of plasma ferritin, transferrin or iron as primary diagnostic parameters for iron homeostasis was only rarely described in other ENU mutagenesis projects. In summary, we successfully established three novel mouse models for the functional analysis of iron metabolism by the means of a phenotype-driven mutagenesis screen.

Acknowledgments We thank Andreas Mayer, Sandra Hoffmann and Elfi Holupirek and our animal caretaker team for technical support.

Funding This work was supported by the German Human Genome Project (DHGP) and the National Genome Research Network (NGFN) (MHdA, EW) and by the German Federal Ministry of Education and Research (Infrafrontier Grant 01KX1012).

Conflict of interest The authors declare that they have no competing interests.

References

Aigner B et al (2009a) Generation of N-ethyl-N-nitrosourea-induced mouse mutants with deviations in plasma enzyme activities as novel organ-specific disease models. Exp Physiol 94:412–421

Aigner B, Rathkolb B, Wolf E (2009b) Generation and analysis of disease-specific mouse models by clinical chemical screening. In: Mitchem BH, Sharnham CL (eds) Clinical chemistry research. Nova Science, Hauppauge, pp 239–259

Aigner B et al (2011) Generation of N-ethyl-N-nitrosourea-induced mouse mutants with deviations in hematological parameters. Mamm Genome 22:495–505. doi:10.1007/s00335-011-9328-4

Andrews NC (2008) Forging a field: the golden age of iron biology. Blood 112:219–230

Barbaric I, Wells S, Russ A, Dear TN (2007) Spectrum of ENU-induced mutations in phenotype-driven and gene-driven screens in the mouse. Environ Mol Mutagen 48:124–142

Beaumont C et al (1995) Mutation in the iron responsive element of the L ferritin mRNA in a family with dominant hyperferritinaemia and cataract. Nat Genet 11:444–446

Benyamin B et al (2009) Common variants in TMPRSS6 are associated with iron status and erythrocyte volume. Nat Genet 41:1173–1175

Bermejo F, Garcia-Lopez S (2009) A guide to diagnosis of iron deficiency and iron deficiency anemia in digestive diseases. World J Gastroenterol 15:4638–4643

Beutler E, Felitti V, Ho NJ, Gelbart T (2002) Relationship of body iron stores to levels of serum ferritin, serum iron, unsaturated iron binding capacity and transferrin saturation in patients with iron storage disease. Acta Haematol 107:145–149

Champy MF et al (2008) Genetic background determines metabolic phenotypes in the mouse. Mamm Genome 19:318–331

Cohen LA et al (2010) Serum ferritin is derived primarily from macrophages through a nonclassical secretory pathway. Blood 116:1574–1584. doi:10.1182/blood-2009-11-253815

Cooperman SS, Meyron-Holtz EG, Olivierre-Wilson H, Ghosh MC, McConnell JP, Rouault TA (2005) Microcytic anemia, erythropoietic protoporphyria, and neurodegeneration in mice with targeted deletion of iron-regulatory protein 2. Blood 106:1084–1091

Cordes SP (2005) N-ethyl-N-nitrosourea mutagenesis: boarding the mouse mutant express. Microbiol Mol Biol Rev 69:426–439

Cozzi A et al (2013) Human L-ferritin deficiency is characterized by idiopathic generalized seizures and atypical restless leg syndrome. J Exp Med 210:1779–1791. doi:10.1084/jem.20130315

Du X et al (2008) The serine protease TMPRSS6 is required to sense iron deficiency. Science 320:1088–1092

Ferreira C, Santambrogio P, Martin ME, Andrieu V, Feldmann G, Henin D, Beaumont C (2001) H ferritin knockout mice: a model of hyperferritinemia in the absence of iron overload. Blood 98:525–532

Gailus-Durner V et al (2005) Introducing the German mouse clinic: open access platform for standardized phenotyping. Nat Methods 2:403–404

Galy B et al (2005) Altered body iron distribution and microcytosis in mice deficient in iron regulatory protein 2 (IRP2). Blood 106:2580–2589

Girelli D, Corrocher R, Bisceglia L, Olivieri O, De Franceschi L, Zelante L, Gasparini P (1995) Molecular basis for the recently described hereditary hyperferritinemia-cataract syndrome: a mutation in the iron-responsive element of ferritin L-subunit gene (the "Verona mutation"). Blood 86:4050–4053

Greth A et al (2012) A novel ENU-mutation in ankyrin-1 disrupts malaria parasite maturation in red blood cells of mice. PLoS One 7:e38999. doi:10.1371/journal.pone.0038999

Heruth DP et al (2010) Mutation in erythroid specific transcription factor KLF1 causes Hereditary Spherocytosis in the Nan hemolytic anemia mouse model. Genomics 96:303–307

Hrabé de Angelis M et al (2000) Genome-wide, large-scale production of mutant mice by ENU mutagenesis. Nat Genet 25:444–447

Hrabé de Angelis M, Michel D, Wagner S, Becker S, Beckers J (2007) Chemical mutagenesis in mice. In: Fox JG, Barthold SW, Davisson MT, Newcomer CE, Quimby FW, Smith AL (eds) The mouse in biomedical research, vol. 1. History, wild mice, and genetics, 2 edn edn. Academic Press, Burlington, pp 225–260

Huang H et al (2013) A deep intronic mutation in the ankyrin-1 gene causes diminished protein expression resulting in hemolytic anemia in mice. G3 (Bethesda) 3:1687–1695. doi:10.1534/g3.113.007013

Kannengiesser C et al (2009) A new missense mutation in the L ferritin coding sequence associated with elevated levels of glycosylated ferritin in serum and absence of iron overload. Haematologica 94:335–339. doi:10.3324/haematol.2008.000125

Keays DA, Clark TG, Campbell TG, Broxholme J, Valdar W (2007) Estimating the number of coding mutations in genotypic and phenotypic driven N-ethyl-N-nitrosourea (ENU) screens: revisited. Mamm Genome 18:123–124

Klempt M, Rathkolb B, Aigner B, Wolf E (2006) Clinical chemical screen. In: Chambon P, Brown S, Hrabé de Angelis M (eds) Standards of mouse model phenotyping. Wiley-VCH, Weinheim, pp 87–107

Knovich MA, Storey JA, Coffman LG, Torti SV, Torti FM (2009) Ferritin for the clinician. Blood Rev 23:95–104

Krieg L, Milstein O, Krebs P, Xia Y, Beutler B, Du X (2011) Mutation of the gastric hydrogen-potassium ATPase alpha subunit causes iron-deficiency anemia in mice. Blood 118:6418–6425. doi:10.1182/blood-2011-04-350082

Lambe T et al (2009) Identification of a Steap3 endosomal targeting motif essential for normal iron metabolism. Blood 113:1805–1808

Loeb WF, Quimby FW (1999) The clinical chemistry of laboratory animals, Second edition edn. Taylor & Francis, Philadelphia

MacKenzie EL, Iwasaki K, Tsuji Y (2008) Intracellular iron transport and storage: from molecular mechanisms to health implications. Antioxid Redox Signal 10:997–1030. doi:10.1089/ars.2007.1893

McLaren CE et al (2011) Genome-wide association study identifies genetic loci associated with iron deficiency. PLoS One 6:e17390. doi:10.1371/journal.pone.0017390

McLaren CE et al (2012) Associations between single nucleotide polymorphisms in iron-related genes and iron status in multiethnic populations. PLoS One 7:e38339. doi:10.1371/journal.pone.0038339

Mohr M, Klempt M, Rathkolb B, Hrabé de Angelis M, Wolf E, Aigner B (2004) Hypercholesterolemia in ENU-induced mouse mutants. J Lipid Res 45:2132–2137

Muckenthaler M et al (2003) Relationships and distinctions in iron-regulatory networks responding to interrelated signals. Blood 101:3690–3698

Muckenthaler MU, Galy B, Hentze MW (2008) Systemic iron homeostasis and the iron-responsive element/iron-regulatory protein (IRE/IRP) regulatory network. Annu Rev Nutr 28:197–213

Nicklas W, Baneux P, Boot R, Decelle T, Deeny AA, Fumanelli M, Illgen-Wilcke B (2002) Recommendations for the health monitoring of rodent and rabbit colonies in breeding and experimental units. Lab Anim 36:20–42

Nolan PM et al (2000) A systematic, genome-wide, phenotype-driven mutagenesis programme for gene function studies in the mouse. Nat Genet 25:440–443

Rank G et al (2009) Novel roles for erythroid Ankyrin-1 revealed through an ENU-induced null mouse mutant. Blood 113:3352–3362

Rathkolb B et al (2000) The clinical-chemical screen in the Munich ENU mouse mutagenesis project: screening for clinically relevant phenotypes. Mamm Genome 11:543–546

Robledo RF et al (2010) Analysis of novel sph (spherocytosis) alleles in mice reveals allele-specific loss of band 3 and adducin in alpha-spectrin-deficient red cells. Blood 115:1804–1814

Siatecka M, Sahr KE, Andersen SG, Mezei M, Bieker JJ, Peters LL (2010) Severe anemia in the Nan mutant mouse caused by sequence-selective disruption of erythroid Kruppel-like factor. Proc Natl Acad Sci USA 107:15151–15156

Takahasi KR, Sakuraba Y, Gondo Y (2007) Mutational pattern and frequency of induced nucleotide changes in mouse ENU mutagenesis. BMC Mol Biol 8:52

Tanaka T et al (2010) A genome-wide association analysis of serum iron concentrations. Blood 115:94–96. doi:10.1182/blood-2009-07-232496

Thompson K et al (2003) Mouse brains deficient in H-ferritin have normal iron concentration but a protein profile of iron deficiency and increased evidence of oxidative stress. J Neurosci Res 71:46–63

Wang W, Knovich MA, Coffman LG, Torti FM, Torti SV (2010) Serum ferritin: past, present and future. Biochim Biophys Acta 1800:760–769. doi:10.1016/j.bbagen.2010.03.011

Yanagawa T et al (2004) Nrf2 deficiency causes tooth decolourization due to iron transport disorder in enamel organ. Genes Cells 9:641–651

Yuki KE et al (2013) Suppression of hepcidin expression and iron overload mediate Salmonella susceptibility in ankyrin 1 ENU-induced mutant. PLoS One 8:e55331. doi:10.1371/journal.pone.0055331

Zohn IE et al (2007) The flatiron mutation in mouse ferroportin acts as a dominant negative to cause ferroportin disease. Blood 109:4174–4180